

Electronic structure and magnetic properties of **LaFeAsO-** and **FeSe-** based superconductors

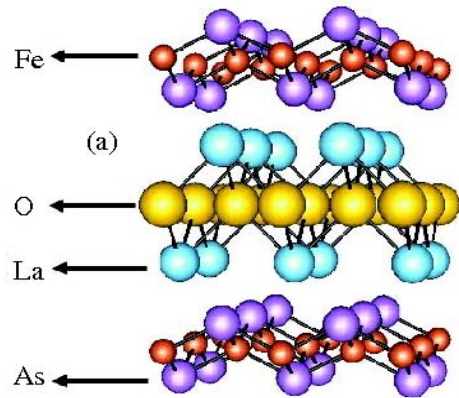
G.E. Grechnev^a, A.S. Panfilov^a, V.A. Desnenko^a, A.V. Fedorchenko^a,
S.L. Gnatchenko^a, D.A. Chareev^{b,c}, O.S. Volkova^c, A.N. Vasiliev^c

^a B. Verkin Institute for Low Temperature Physics and Engineering,
National Academy of Sciences of Ukraine, 61103 Kharkov, Ukraine

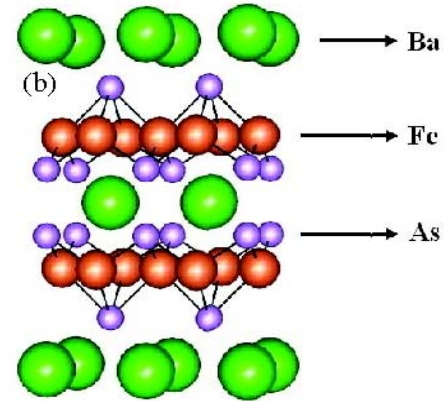
^b Institute of Experimental Mineralogy, Russian Academy of Sciences,
Chernogolovka, Moscow District 142432, Russia

^c Moscow State University, Physics Department, 119991 Moscow, Russia

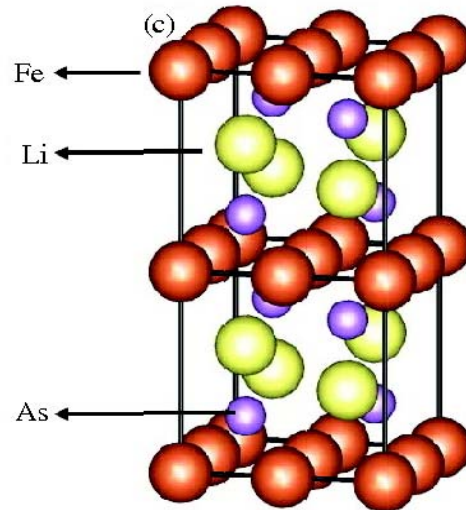
Crystal structures of Fe-based superconductors



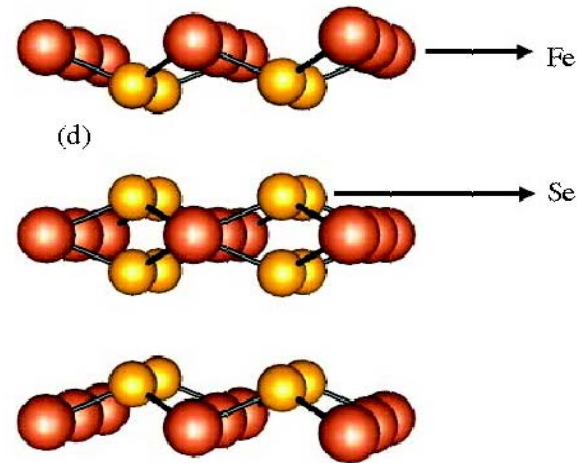
LaFeAsO(F)



Ba(K)Fe₂As₂



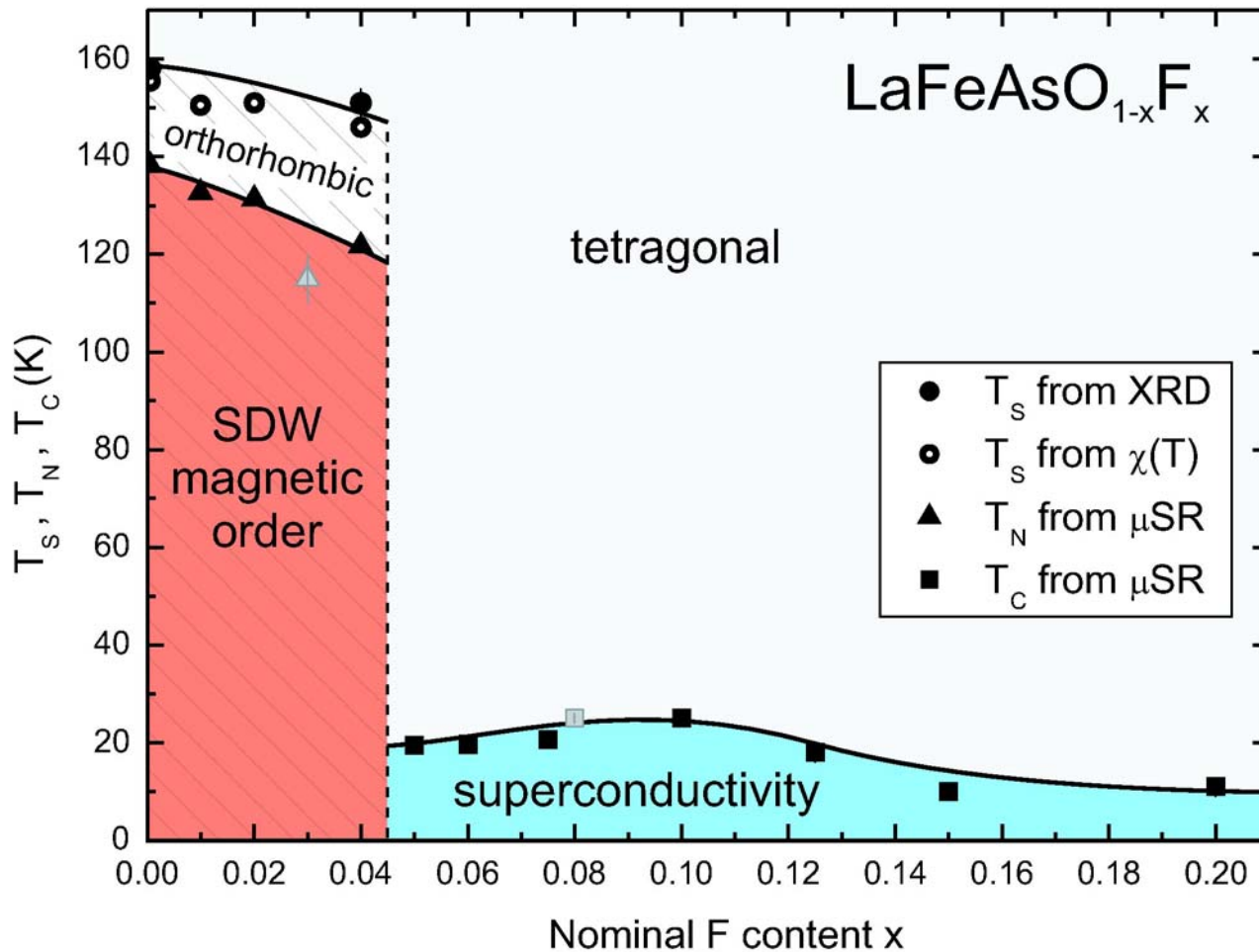
LiFeAs



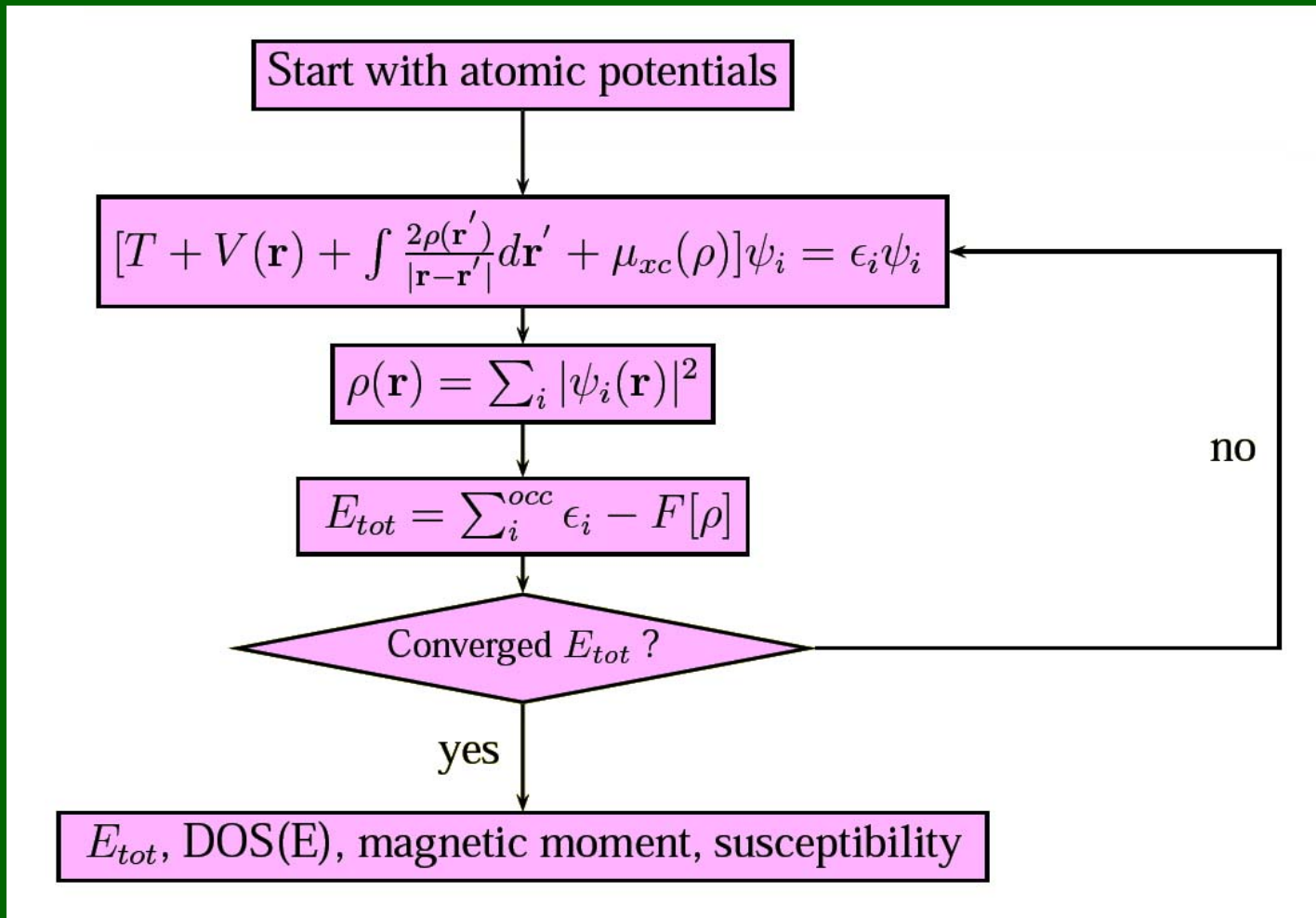
FeSe(Te)

Phase diagram of LaFeAsO(F) system

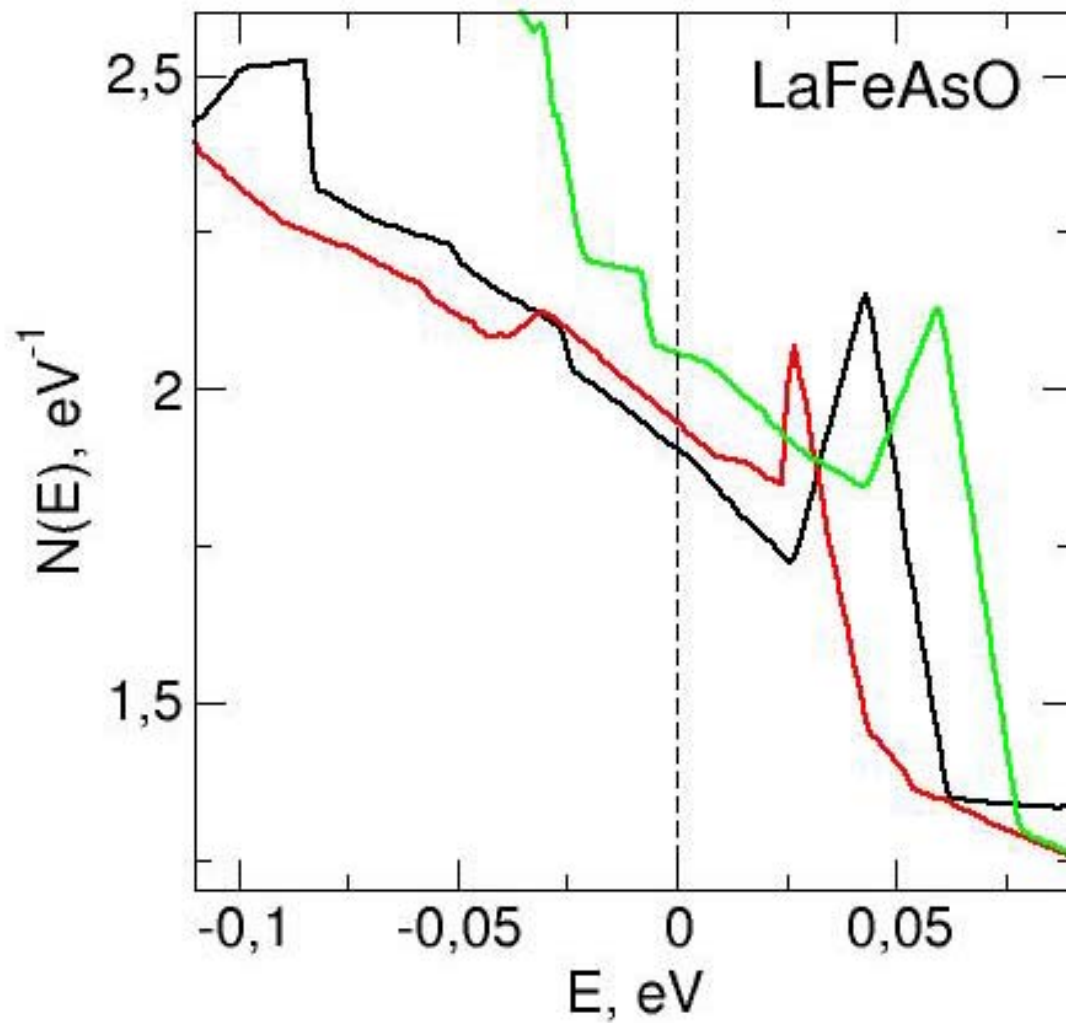
Luetkens et. al. Nature Materials, 8, 305 (2009)



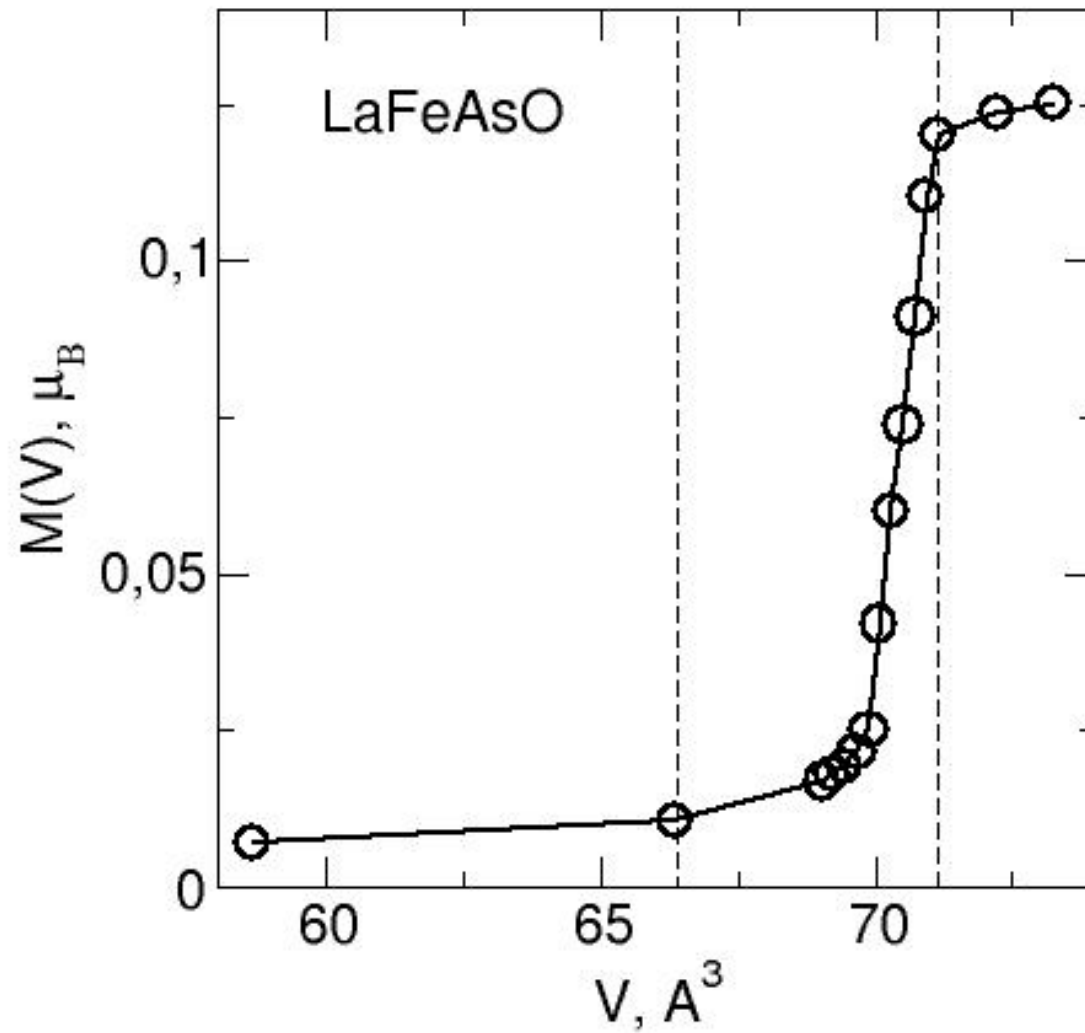
Block diagram of *ab-initio* Full-Potential LMTO calculations within LSDA-DFT theory



Density of states of LaFeAsO(F)

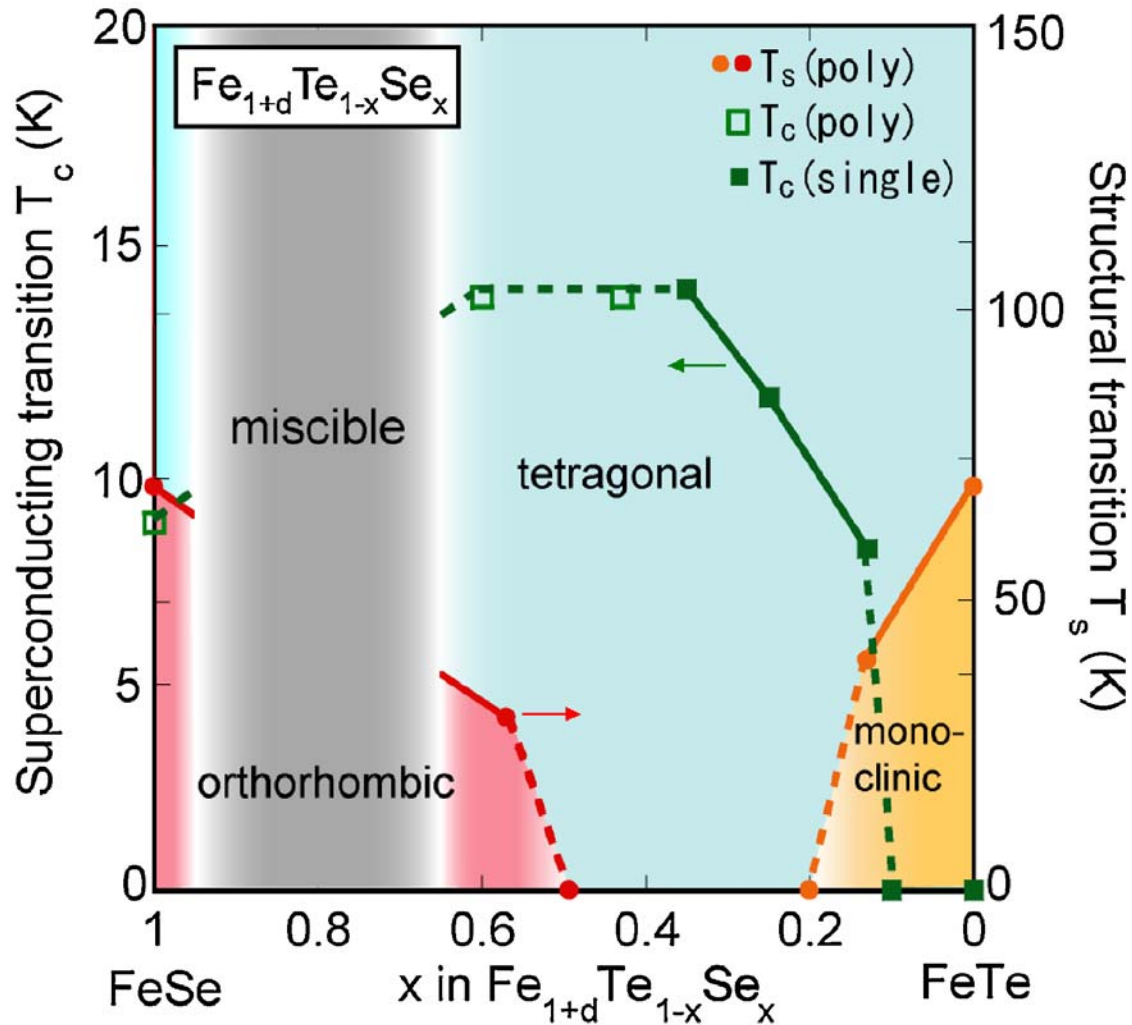


Volume dependence of magnetic moment of LaFeAsO



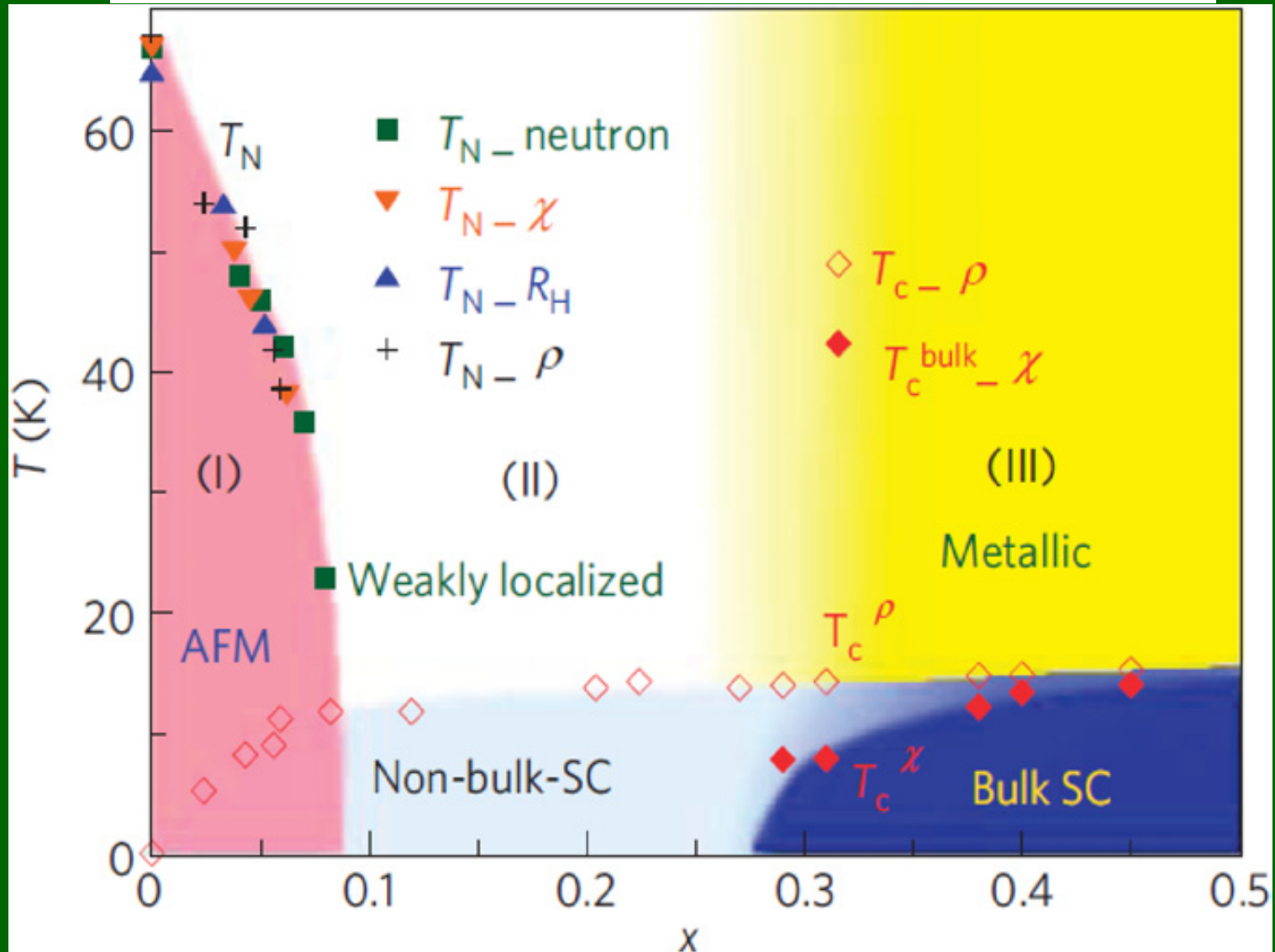
Phase diagram 1 of FeTe(Se) system

Y. MIZUGUCHI and Y. TAKANO, J. Phys. Soc. Japan 79 (2010) 102001

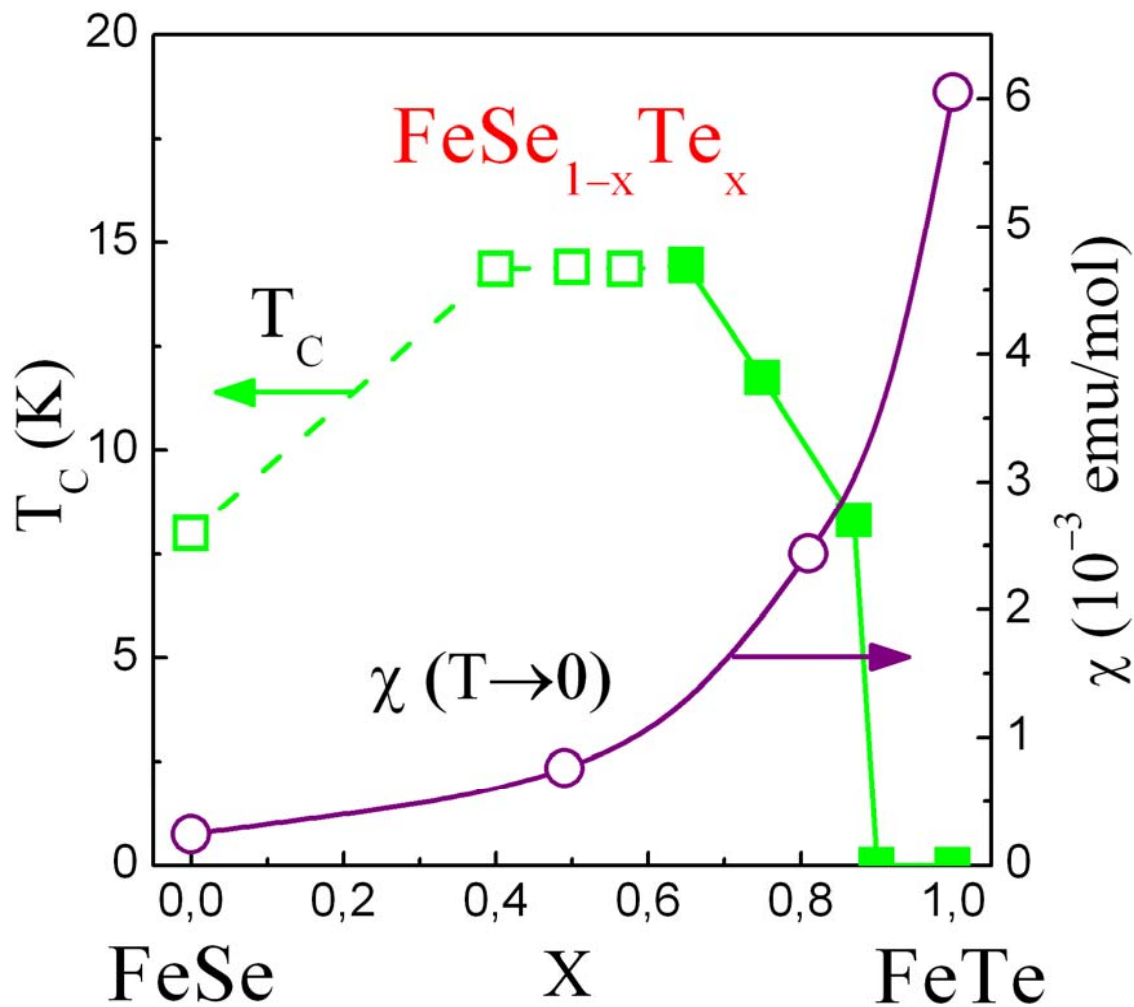


Phase diagram 2 of FeTe(Se) system

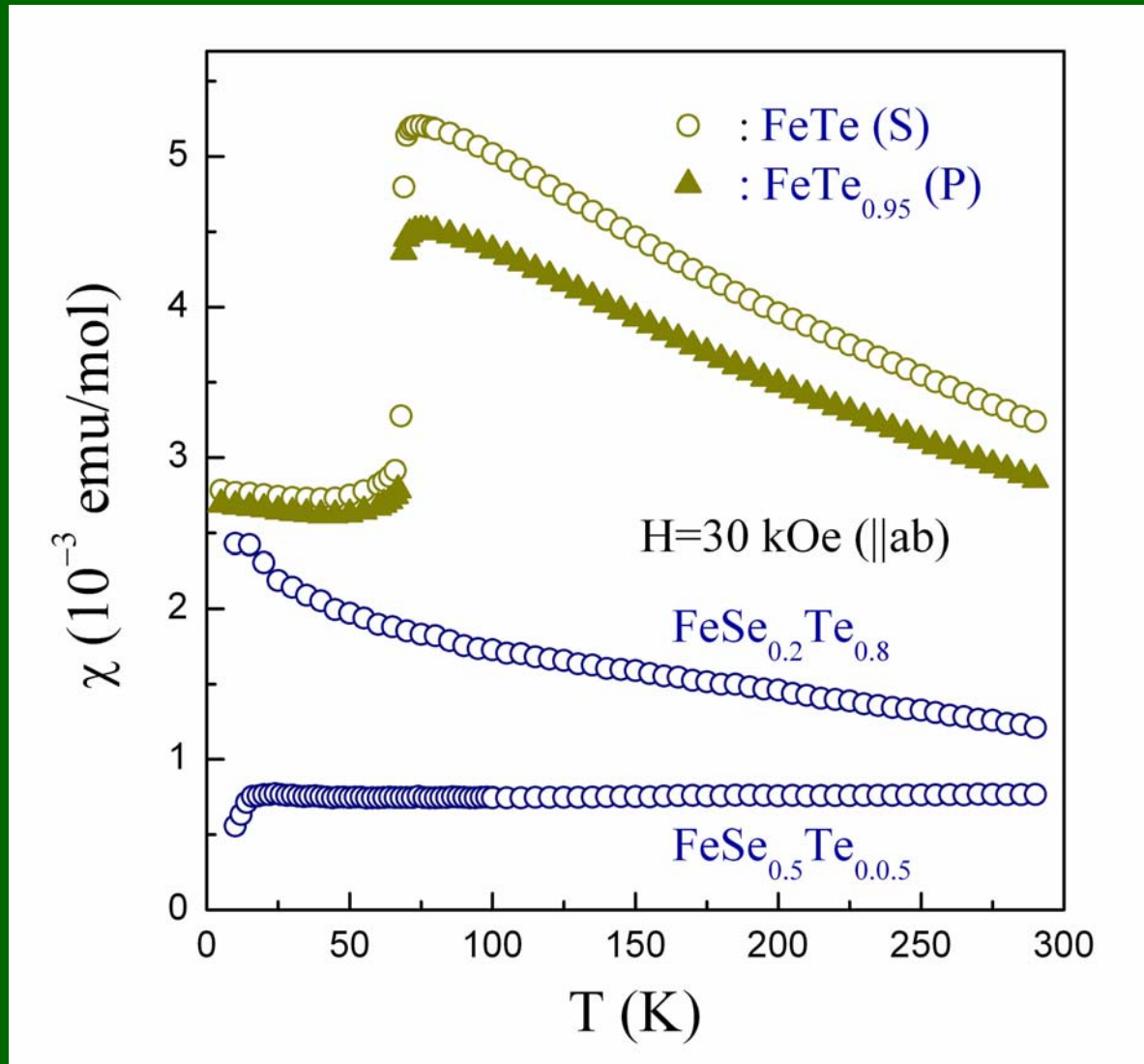
Liu T.J. et. al., Nature Materials, 9, 718 (2010)



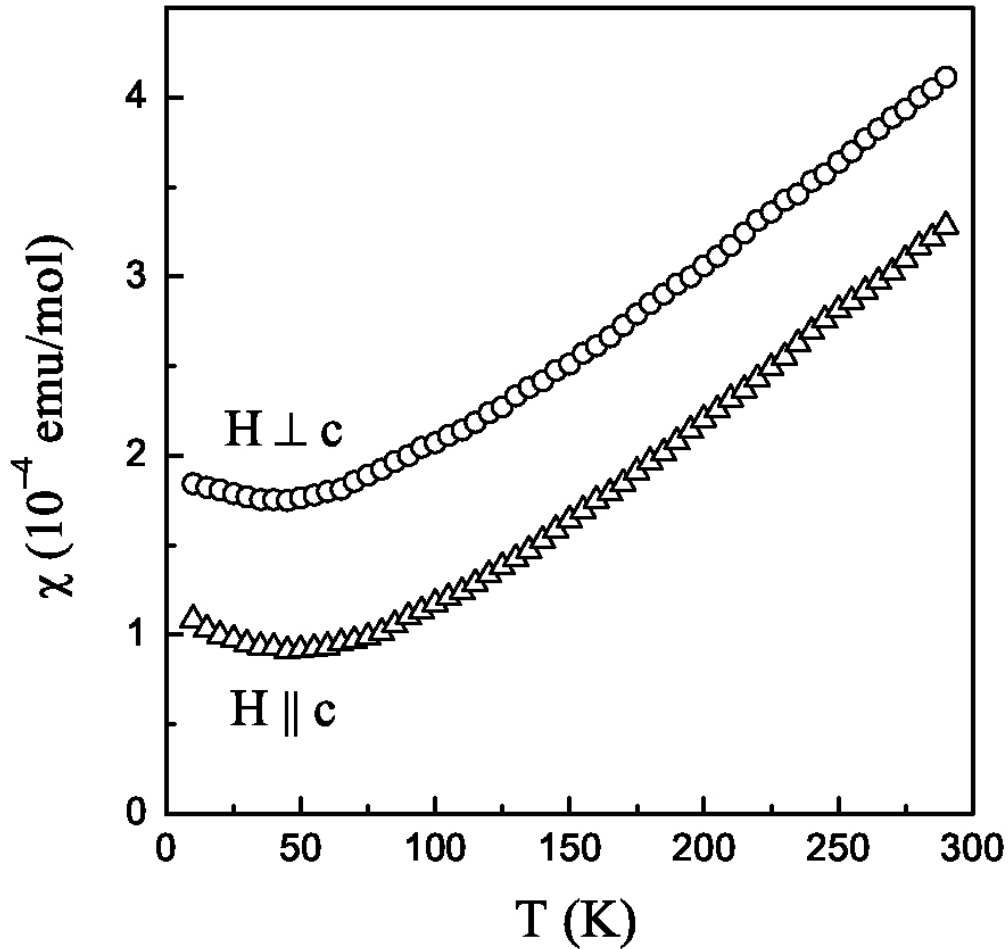
Concentration dependence of T_C and magnetic susceptibility of the normal state



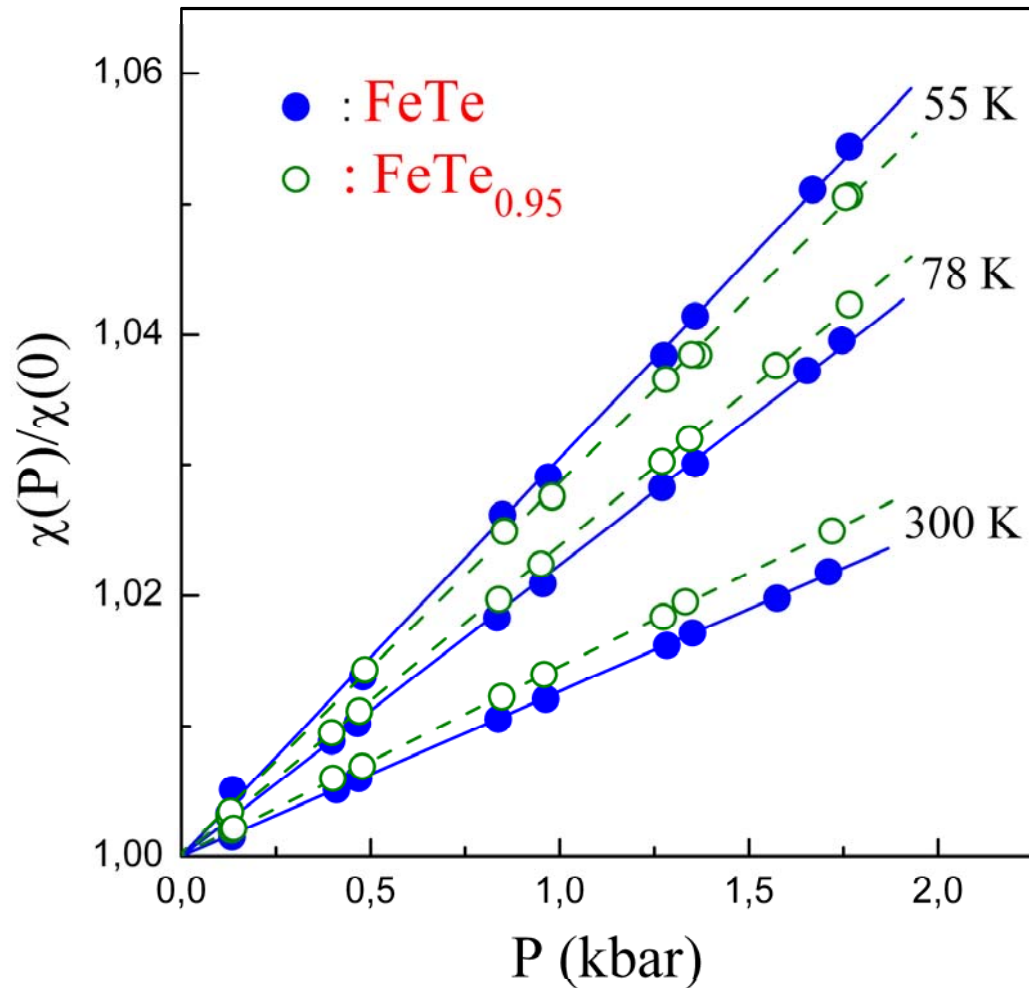
Temperature dependence of magnetic susceptibility of FeSe(Te) compounds



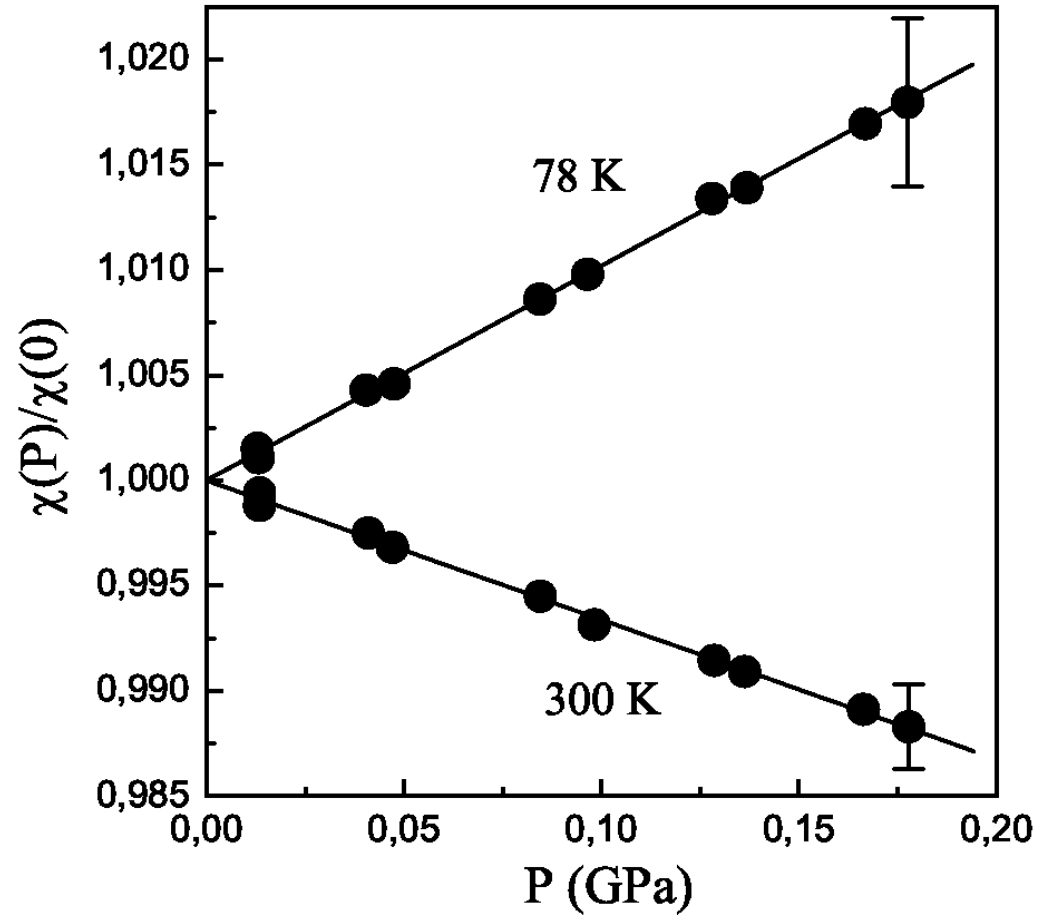
Temperature dependence of the magnetic susceptibility of FeSe



Pressure dependence of the magnetic susceptibility of FeTe



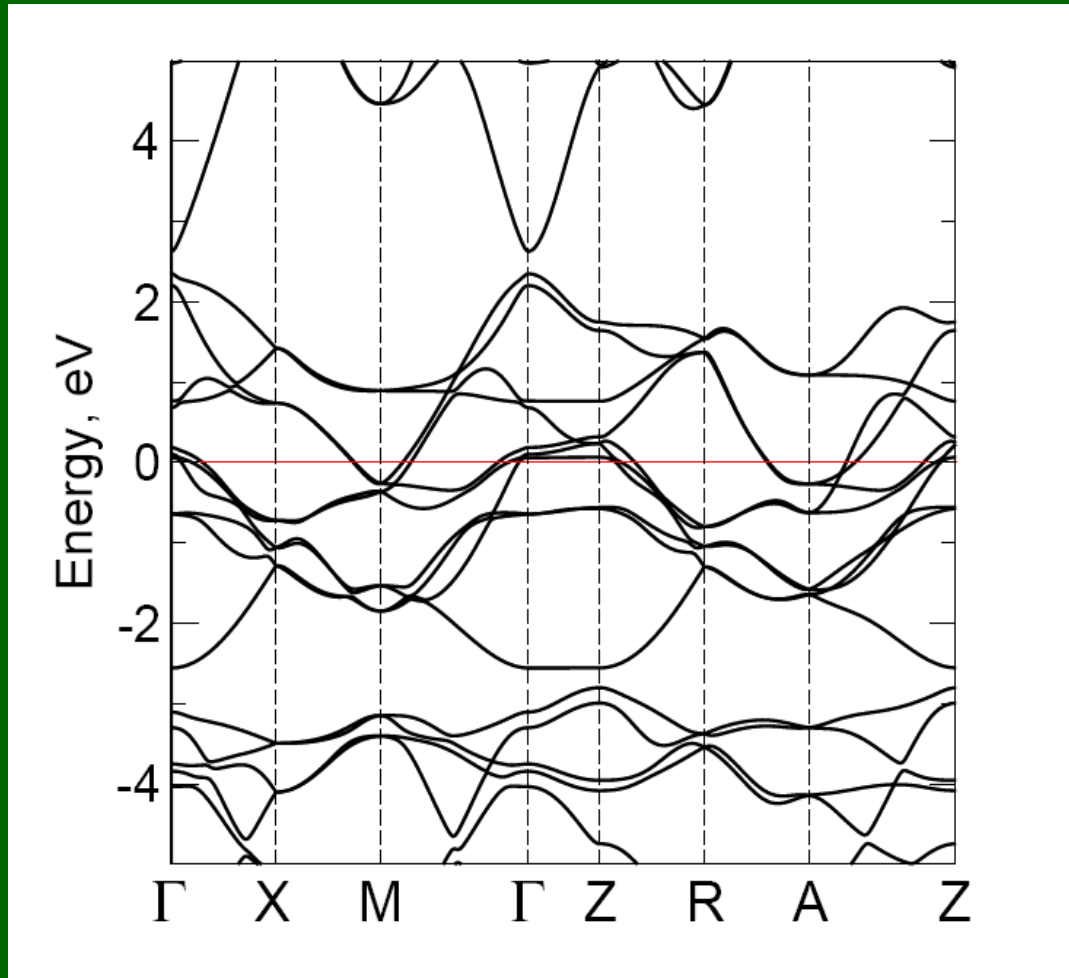
Pressure dependence of the magnetic susceptibility of FeSe



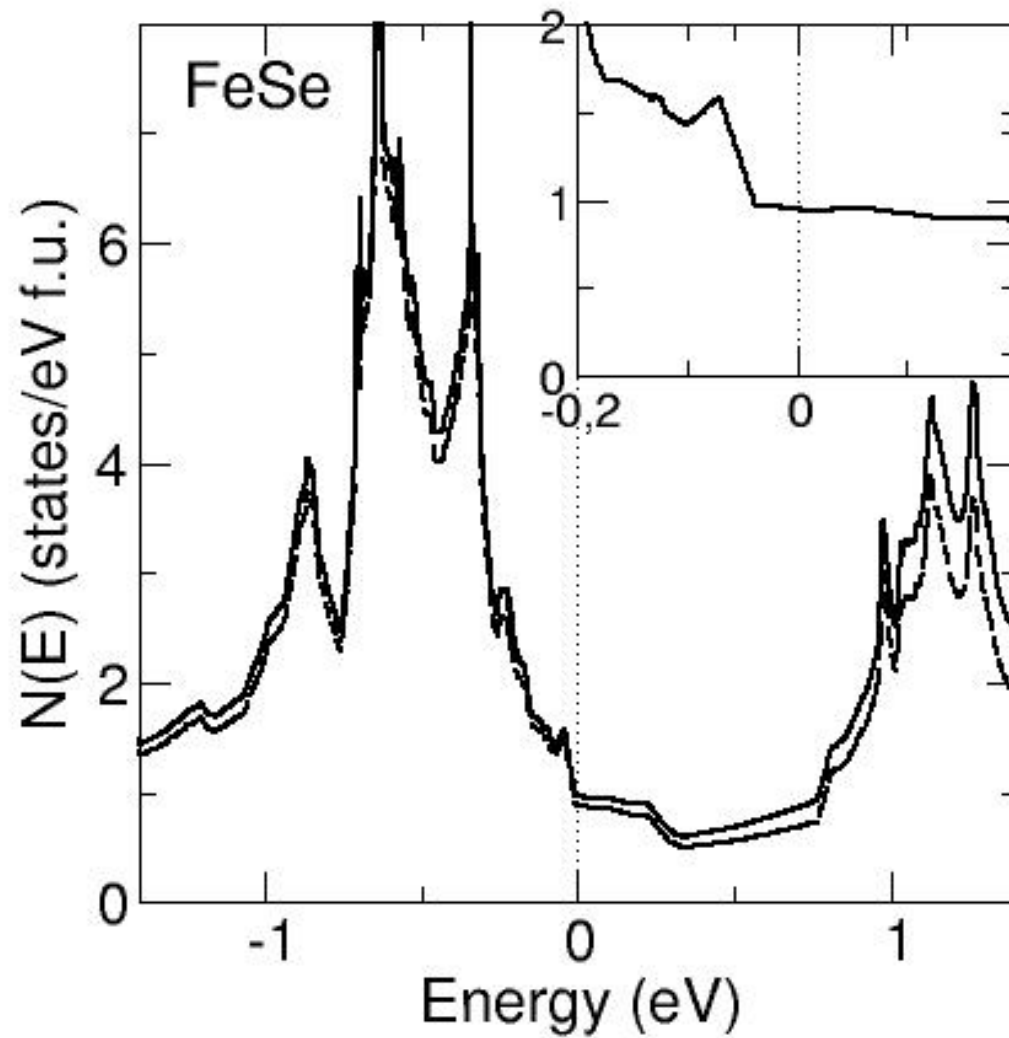
Pressure derivative of the magnetic susceptibility $d \ln \chi / dP$ (10^{-2} GPa^{-1}) for FeSe and FeTe compounds at different temperatures.

	$T(\text{K})$	$d \ln \chi / dP$	
		FeSe	FeTe ^b
experiment:	300	-6.5 ± 1 $\sim -7^a$	13 ± 1
	78	10 ± 3 $\sim 6.5^a$	23 ± 1.5
	20	$\sim 9^a$	
theory:	0	$\simeq 8$	~ 20

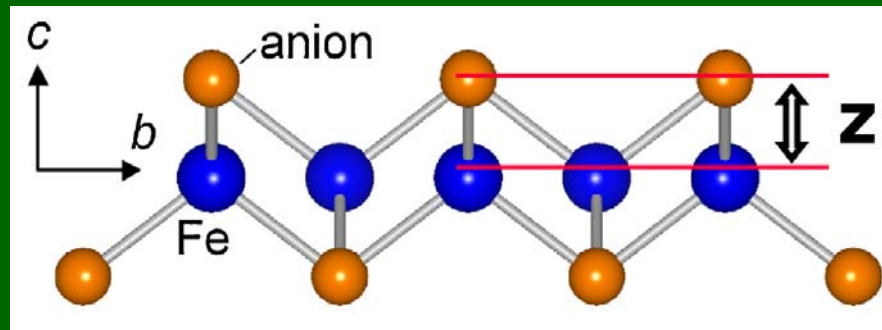
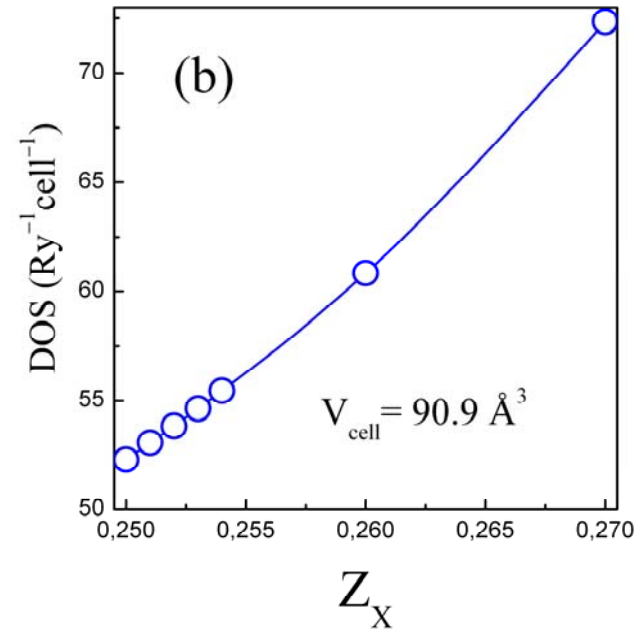
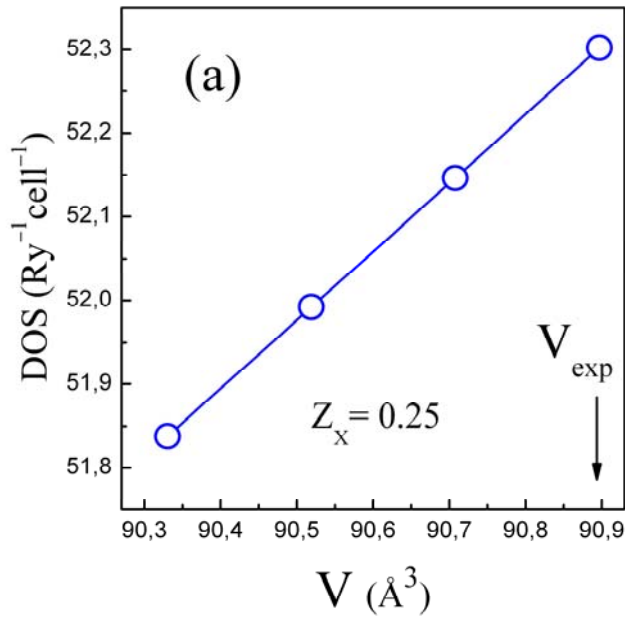
Band structure of FeSe compound



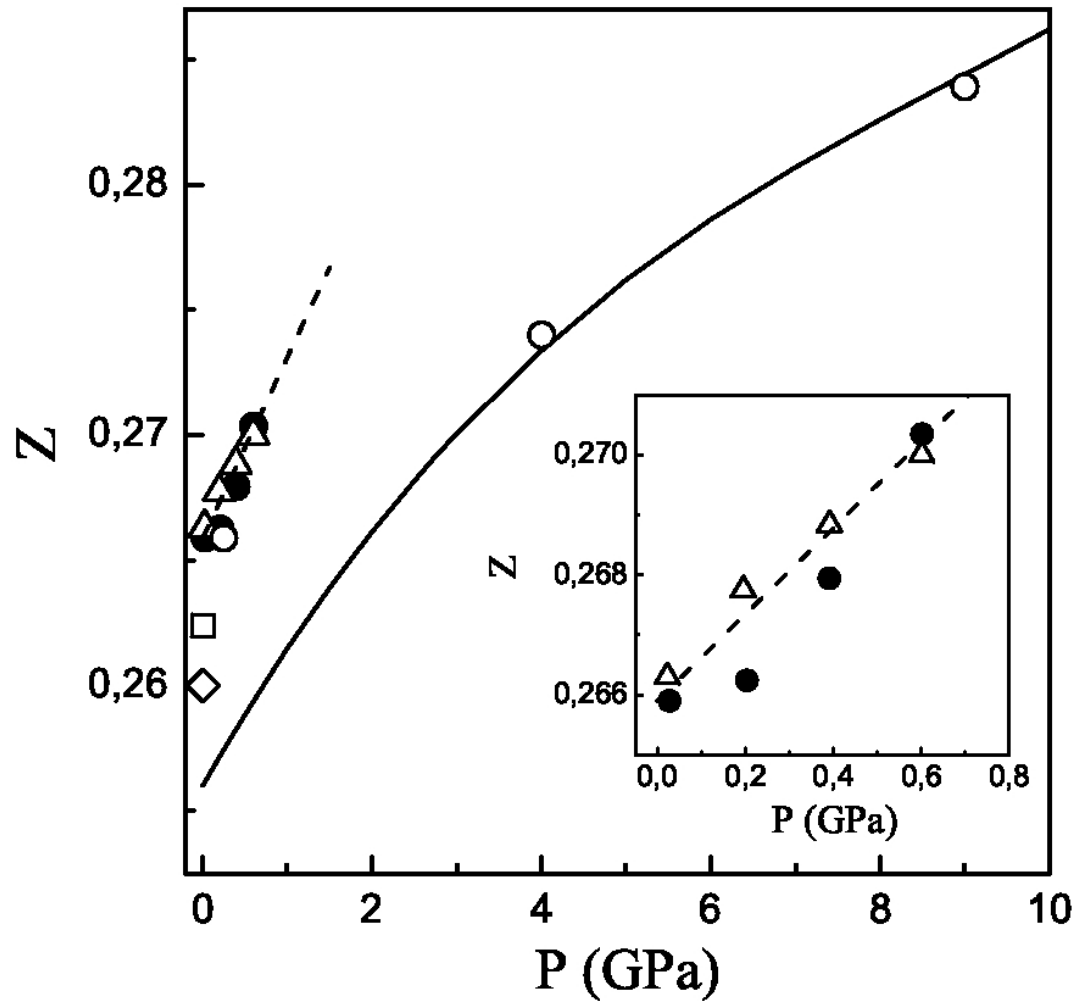
Density of states of FeSe compound

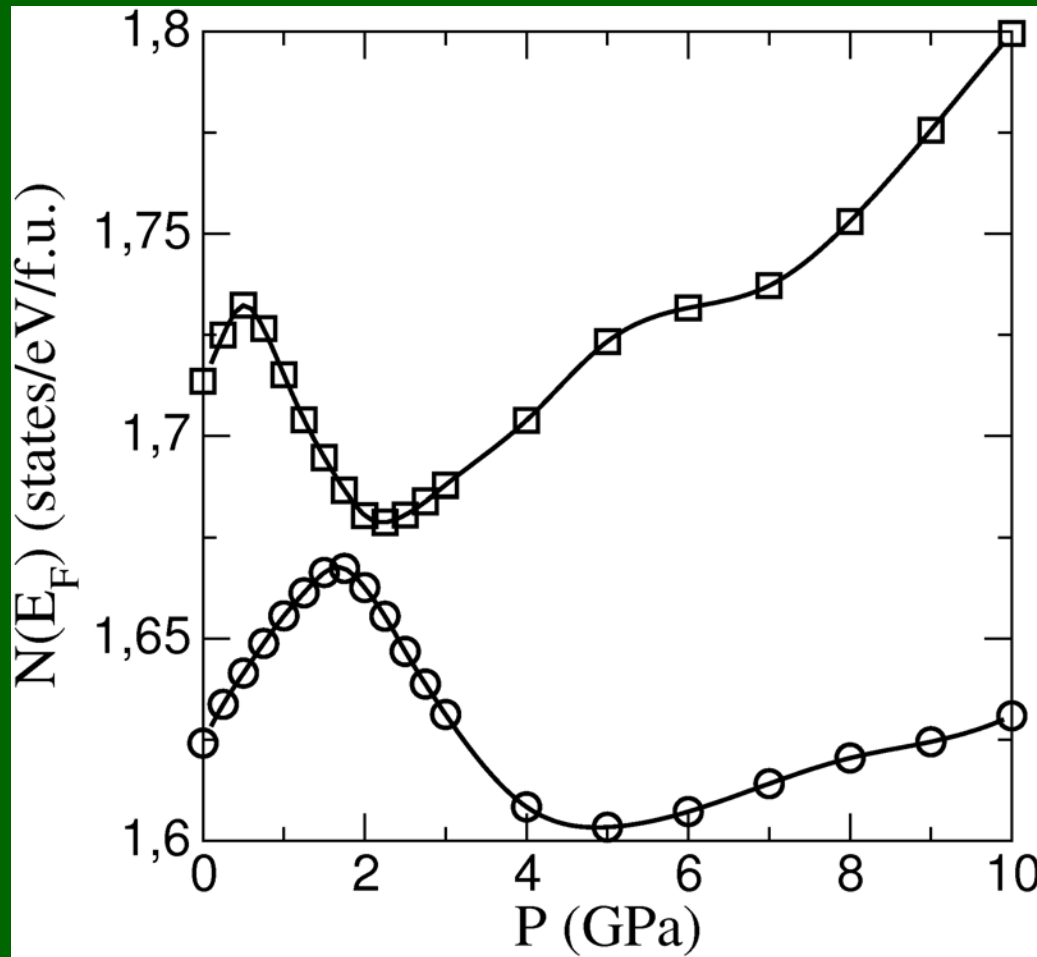


Dependence of density of states at Fermi energy for FeTe on volume and parameter Z



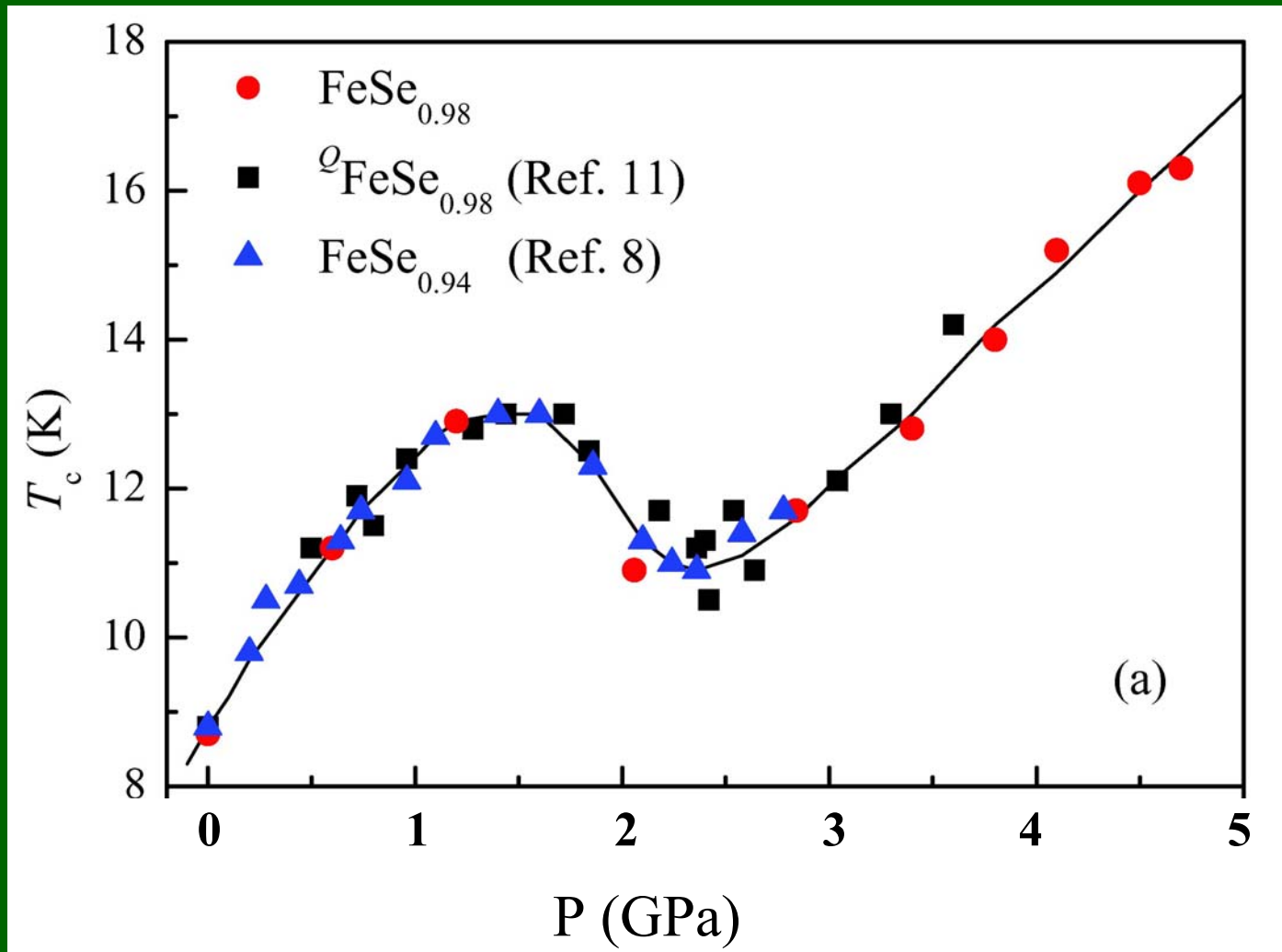
Pressure dependence of the internal chalcogen structural parameter Z for FeSe



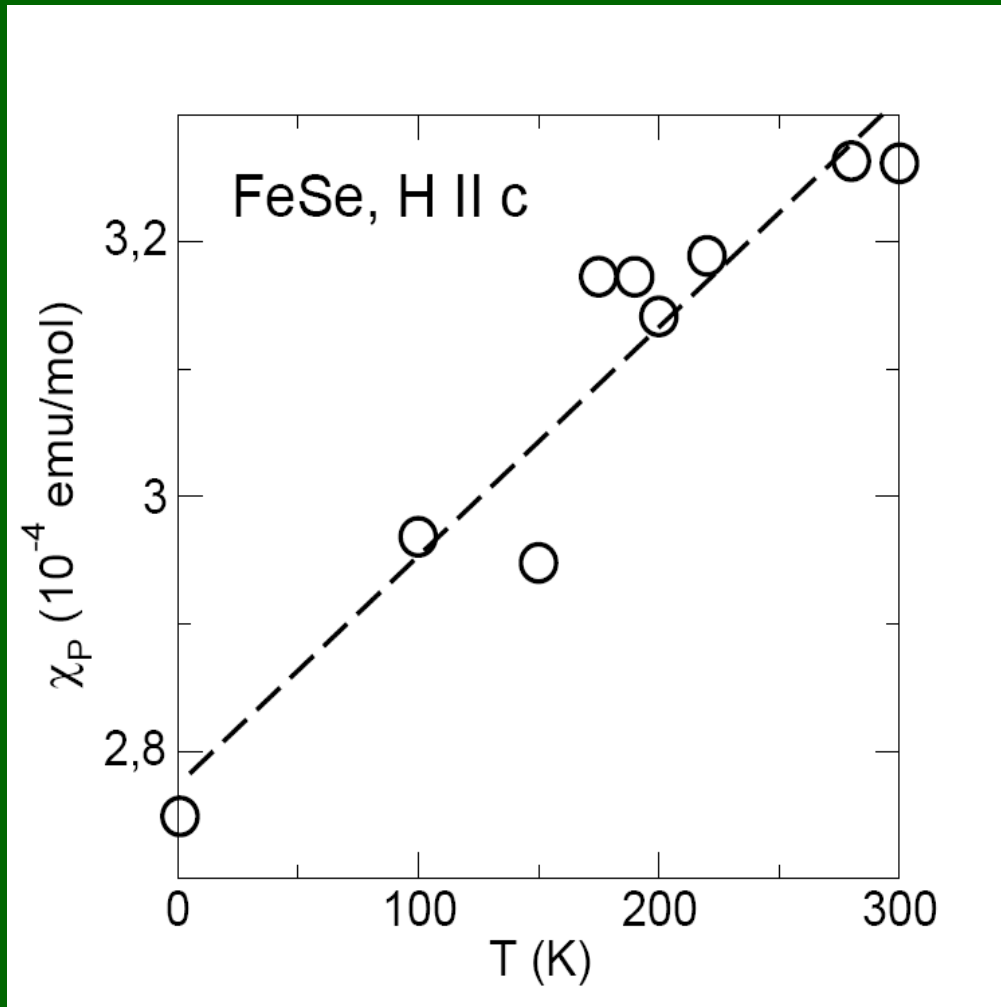


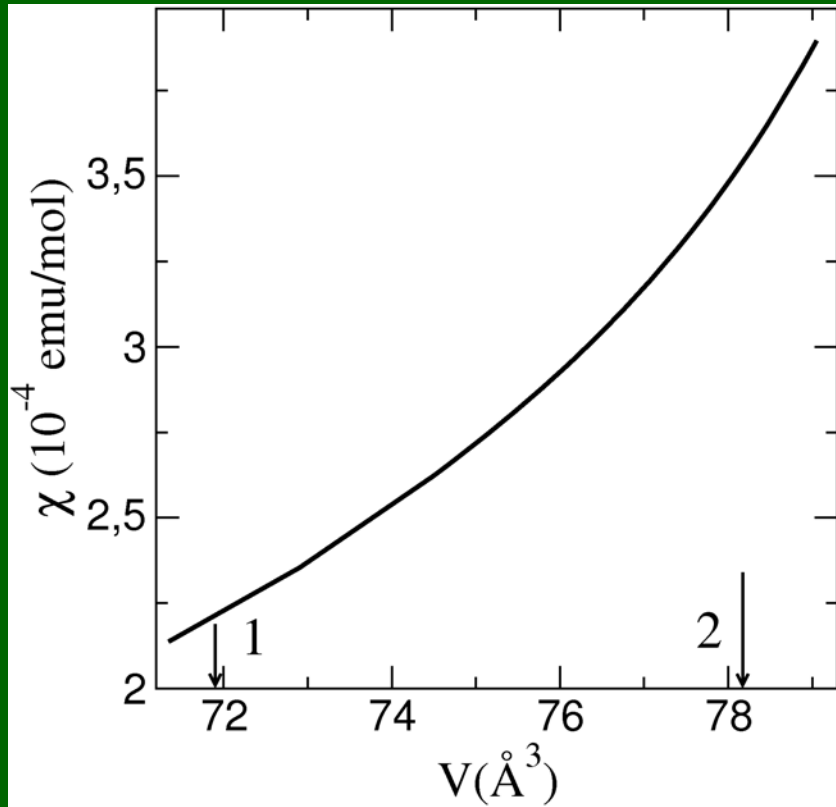
Calculated pressure dependencies of the density of states at the Fermi level for FeSe. (The solid lines are guides for the eye).

Pressure dependence of the superconducting transition temperature of FeSe

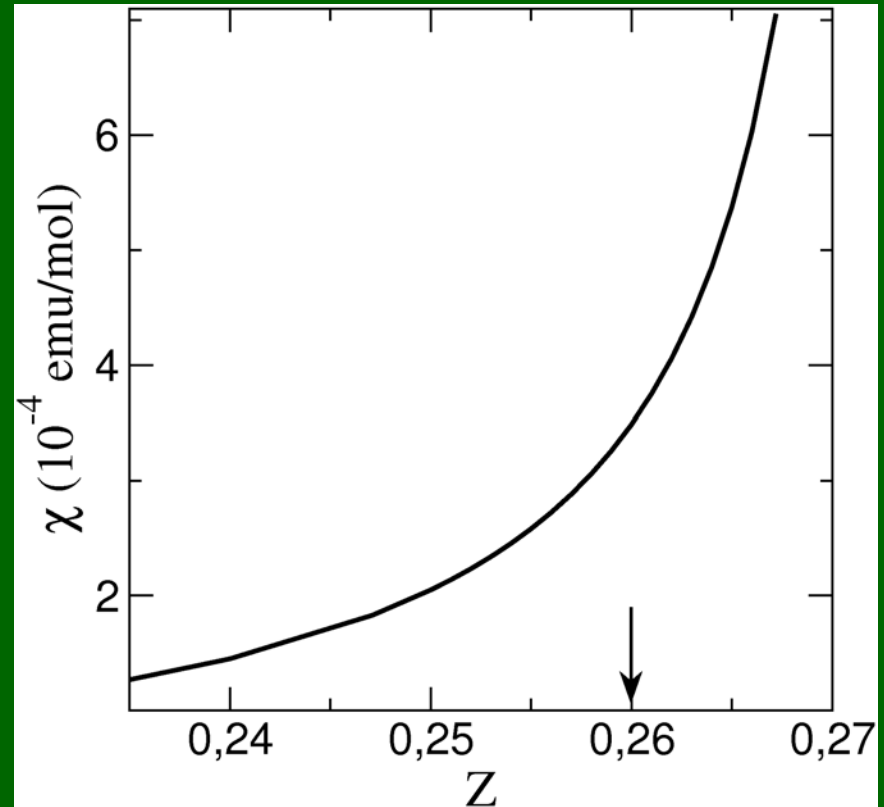


Calculated temperature dependence of the paramagnetic susceptibility of FeSe





Paramagnetic susceptibility of FeSe vs. unit cell volume. Arrows indicate theoretical (1) and experimental (2) volumes.



Paramagnetic susceptibility of FeSe vs. parameter Z for the experimental volume. Arrow indicates the experimental Z .

Main mechanisms for pressure effect on the magnetic susceptibility of FeSe

$$\frac{d \ln \chi}{dP} = \frac{\partial \ln \chi}{\partial \ln V} \times \frac{\partial \ln V}{\partial P} + \frac{\partial \ln \chi}{\partial Z_x} \times \frac{d Z_x}{d P}$$

$$\frac{\partial \ln \chi}{\partial \ln V} \sim 8 \text{ (theory)}, \quad \frac{\partial \ln V}{\partial P} \cong -3 \cdot 10^{-2} \text{ GPa}^{-1} \text{ (exp)}$$

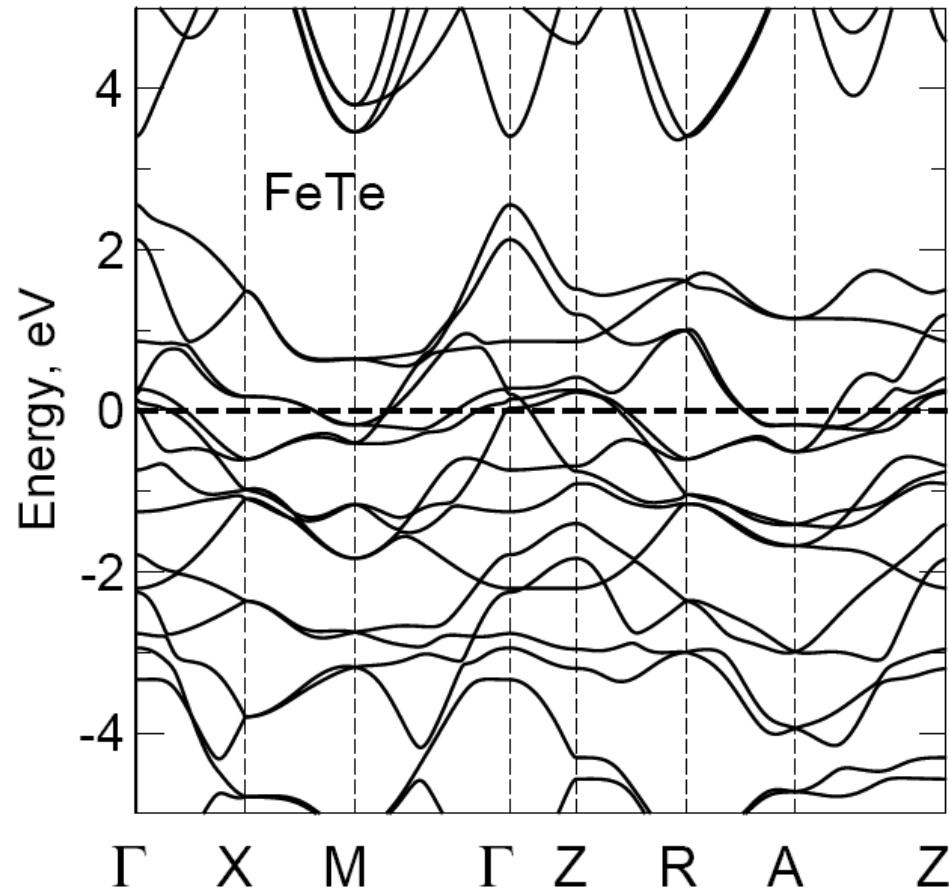
$$\frac{\partial \ln \chi}{\partial Z_x} \sim 65 \text{ (theory)}, \quad \frac{d Z_x}{d P} \approx 0.55 \cdot 10^{-2} \text{ GPa}^{-1} \text{ (fit)}$$

$$\frac{\partial \ln \chi}{\partial \ln V} \times \frac{\partial \ln V}{\partial P} \sim -24 \cdot 10^{-2} \text{ GPa}^{-1}, \quad \frac{\partial \ln \chi}{\partial Z_x} \times \frac{d Z_x}{d P} \sim 36 \cdot 10^{-2} \text{ GPa}^{-1}$$

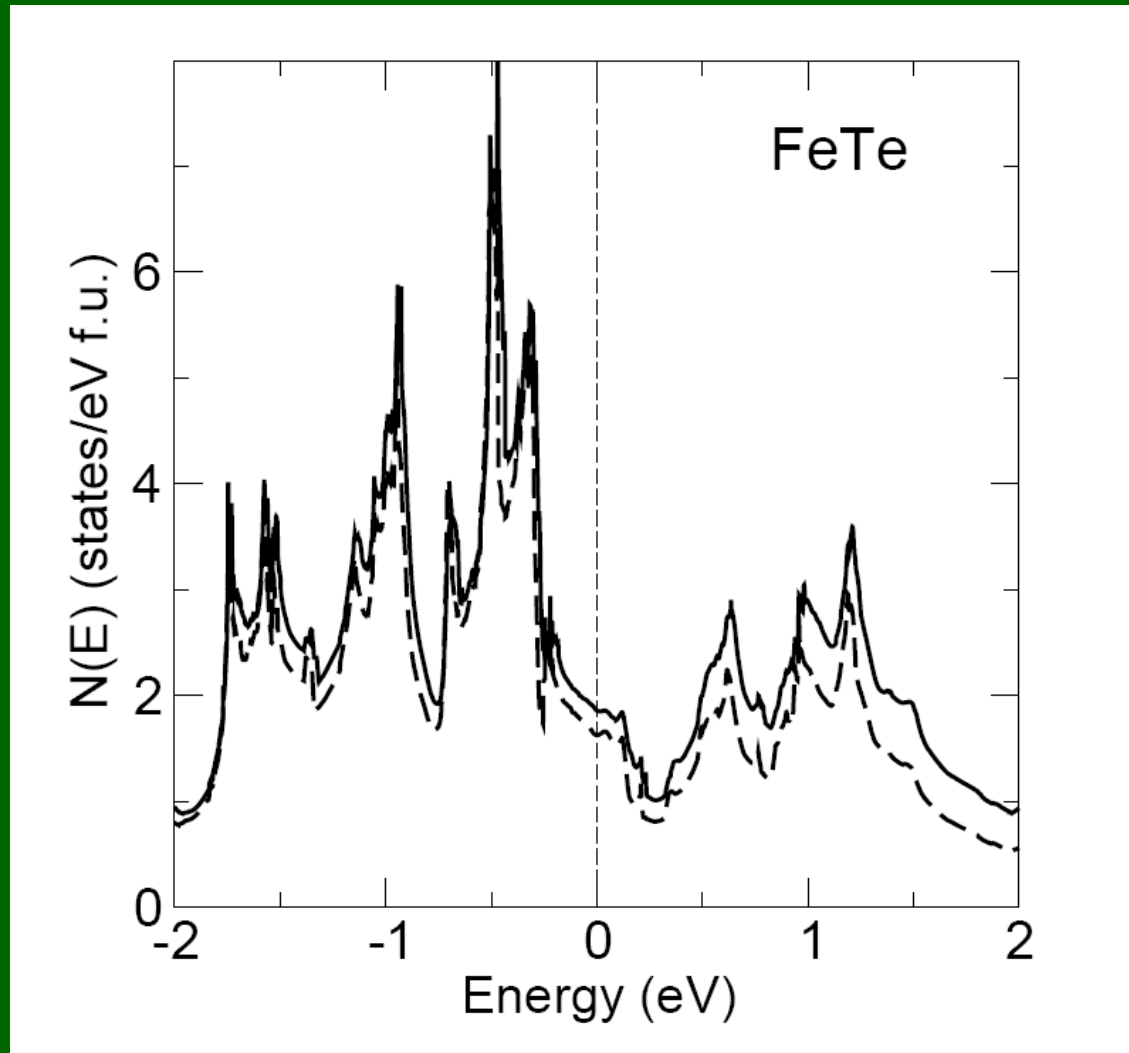
$$\frac{d \ln \chi}{dP} \sim 12 \cdot 10^{-2} \text{ GPa}^{-1} \text{ (theory)}$$

$$\frac{d \ln \chi}{dP} = 8 \cdot 10^{-2} \text{ GPa}^{-1} \text{ (exp)}$$

Band structure of FeTe compound



Density of states of FeTe compound



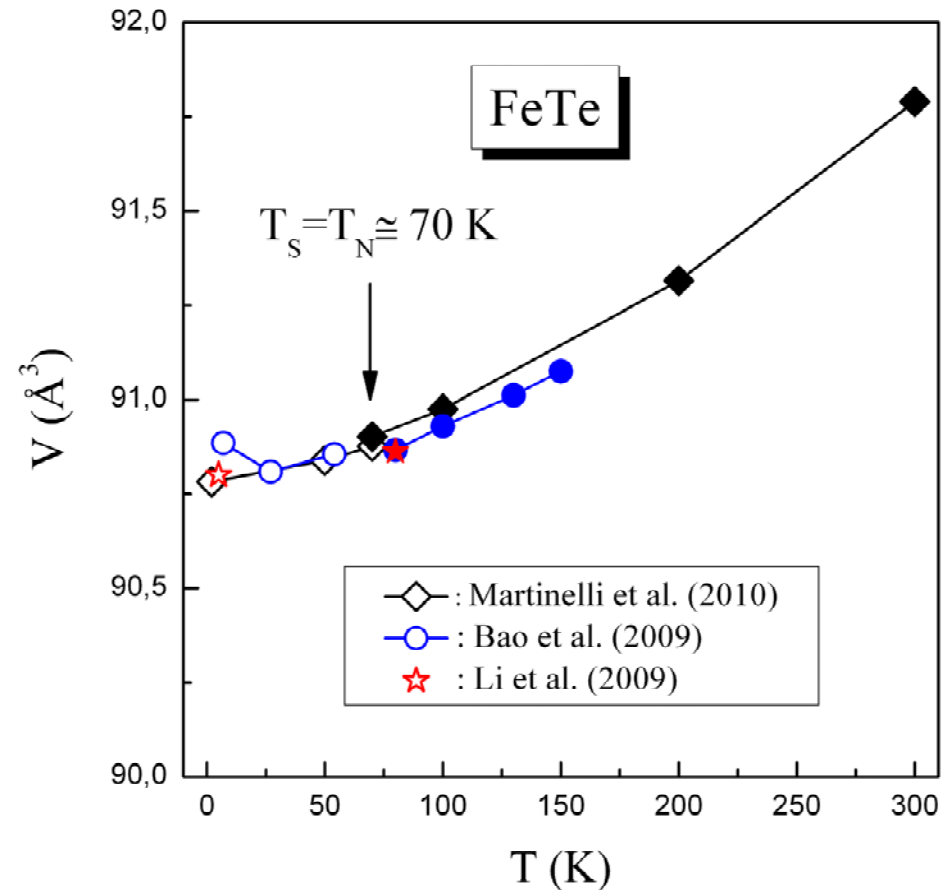
Magnetovolume effect in FeTe

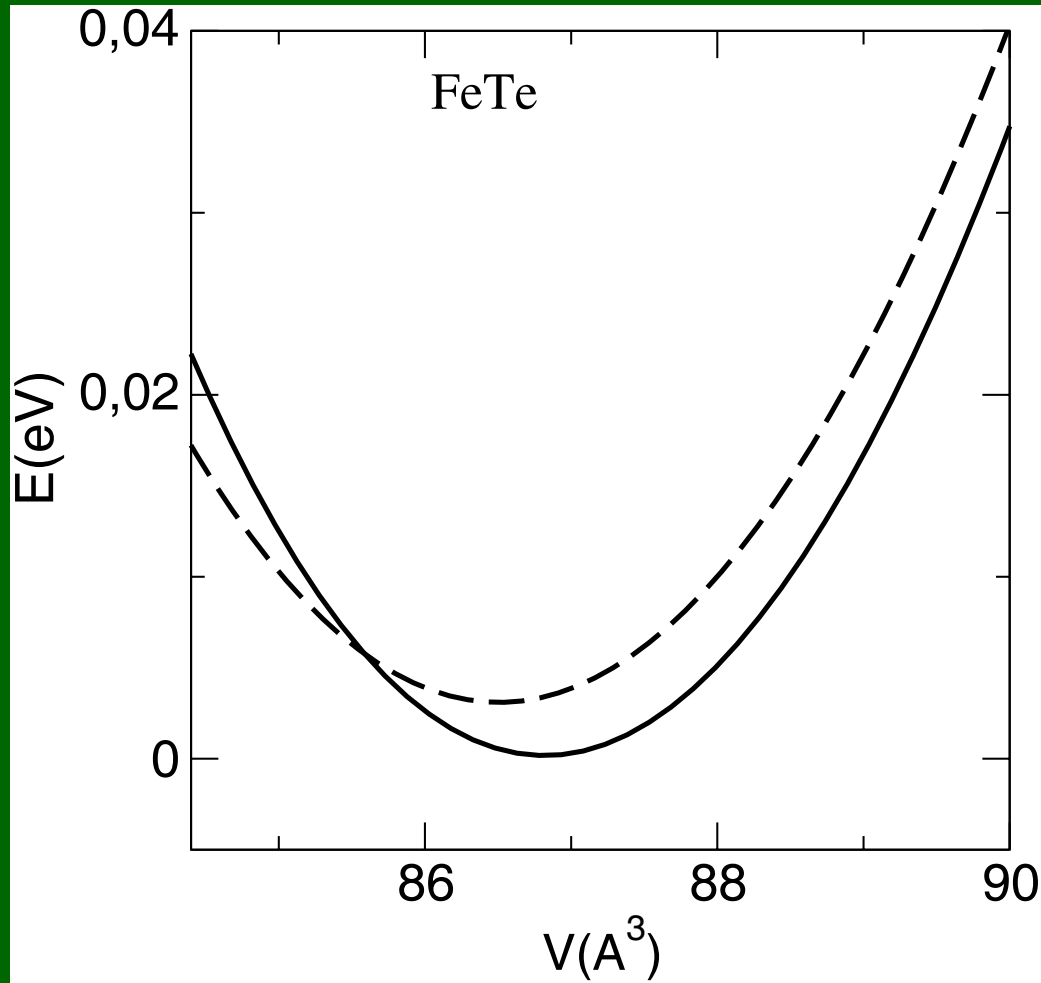
$$\frac{\Delta V}{V} \equiv \omega_m(T) = \frac{C}{B} M^2(T)$$

$$\frac{C}{B} = - \frac{1}{2\chi V} \frac{d \ln \chi}{dP}$$

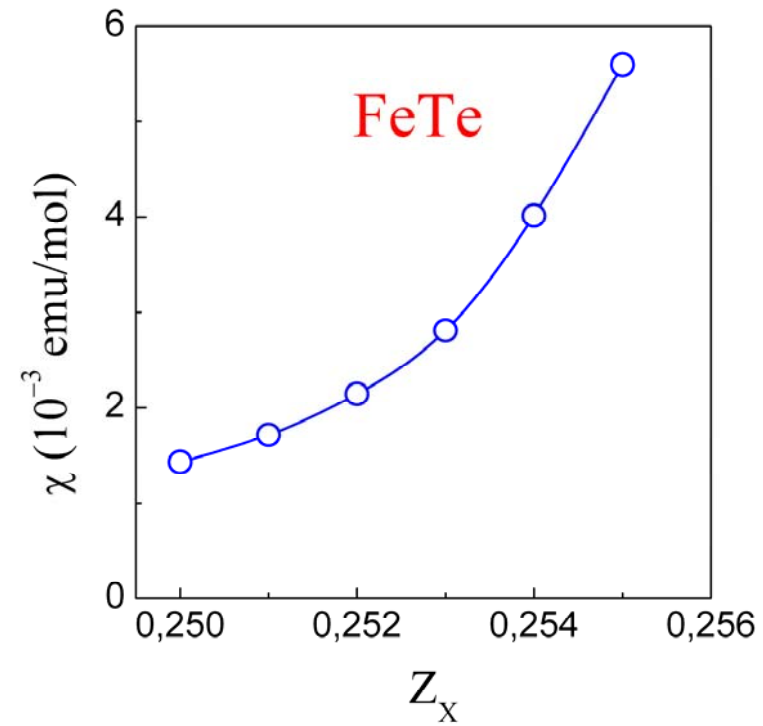
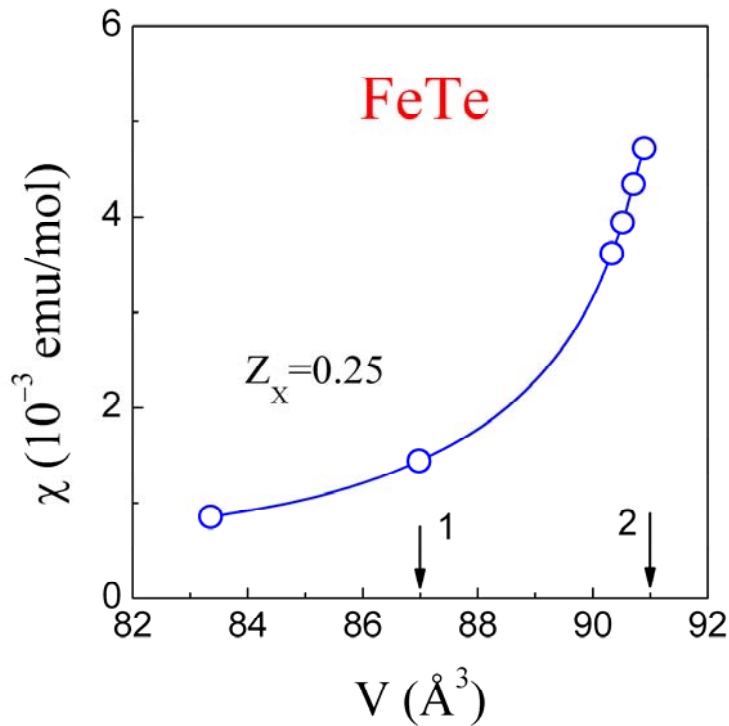
$$M(0) \sim 2\mu_B / \text{Fe}$$

$$\omega_m(0) \sim -0.02 \quad \text{!!!?}$$





- Calculated total energy vs. volume for **FeTe** in the **monoclinic** (solid line) and **tetragonal** (dashed line) structures. The lattice parameters are fixed to experimental ambient pressure values at the phase transition point.



Paramagnetic susceptibility of FeTe versus unit cell volume. The arrows indicate the theoretical (1) and experimental (2) volumes.

Paramagnetic susceptibility of FeTe as function of Z_x for the optimized unit cell volume.

Main mechanisms for pressure effect on the magnetic susceptibility of FeTe

$$\frac{d \ln \chi}{dP} = \frac{\partial \ln \chi}{\partial \ln V} \times \frac{\partial \ln V}{\partial P} + \frac{\partial \ln \chi}{\partial Z_X} \times \frac{d Z_X}{d P}$$

$$\frac{\partial \ln \chi}{\partial \ln V} \sim \mathbf{40} \text{ (theory)}, \quad \frac{\partial \ln V}{\partial P} \cong \mathbf{-3.0} \text{ Mbar}^{-1} \text{ (exp)}$$

$$\frac{\partial \ln \chi}{\partial Z_X} \sim \mathbf{350} \text{ (theory)}, \quad \frac{d Z_X}{d P} \approx \mathbf{0.40} \text{ Mbar}^{-1} \text{ (fit)}$$

$$\frac{\partial \ln \chi}{\partial \ln V} \times \frac{\partial \ln V}{\partial P} \sim \mathbf{-120} \text{ Mbar}^{-1}, \quad \frac{\partial \ln \chi}{\partial Z_X} \times \frac{d Z_X}{d P} \sim \mathbf{140} \text{ Mbar}^{-1}$$

$$\frac{d \ln \chi}{dP} \sim \mathbf{20} \text{ Mbar}^{-1} \text{ (theory)}$$

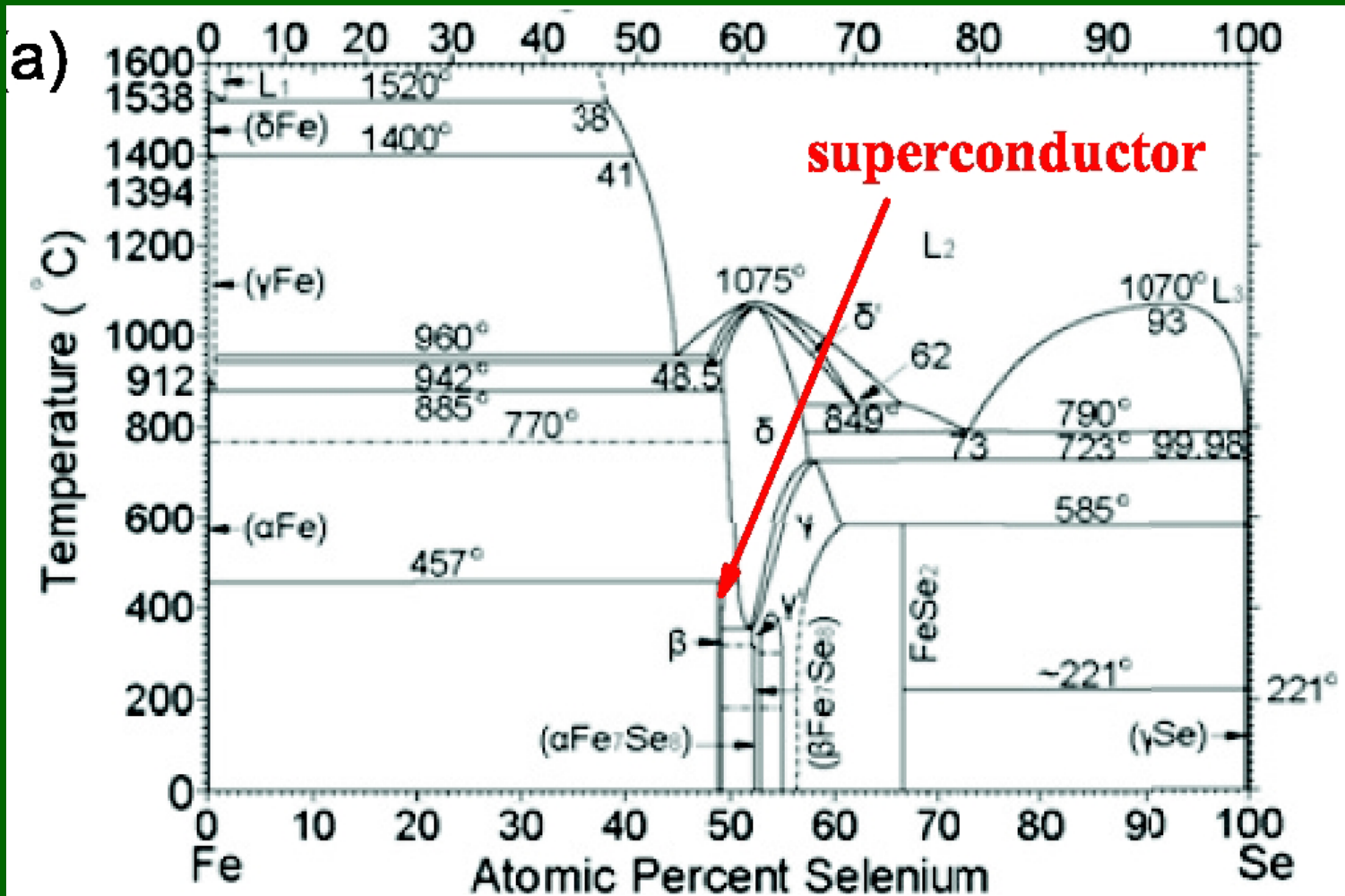
$$\frac{d \ln \chi}{dP} = \mathbf{20} \div \mathbf{25} \text{ Mbar}^{-1} \text{ (exp)}$$

Conclusions

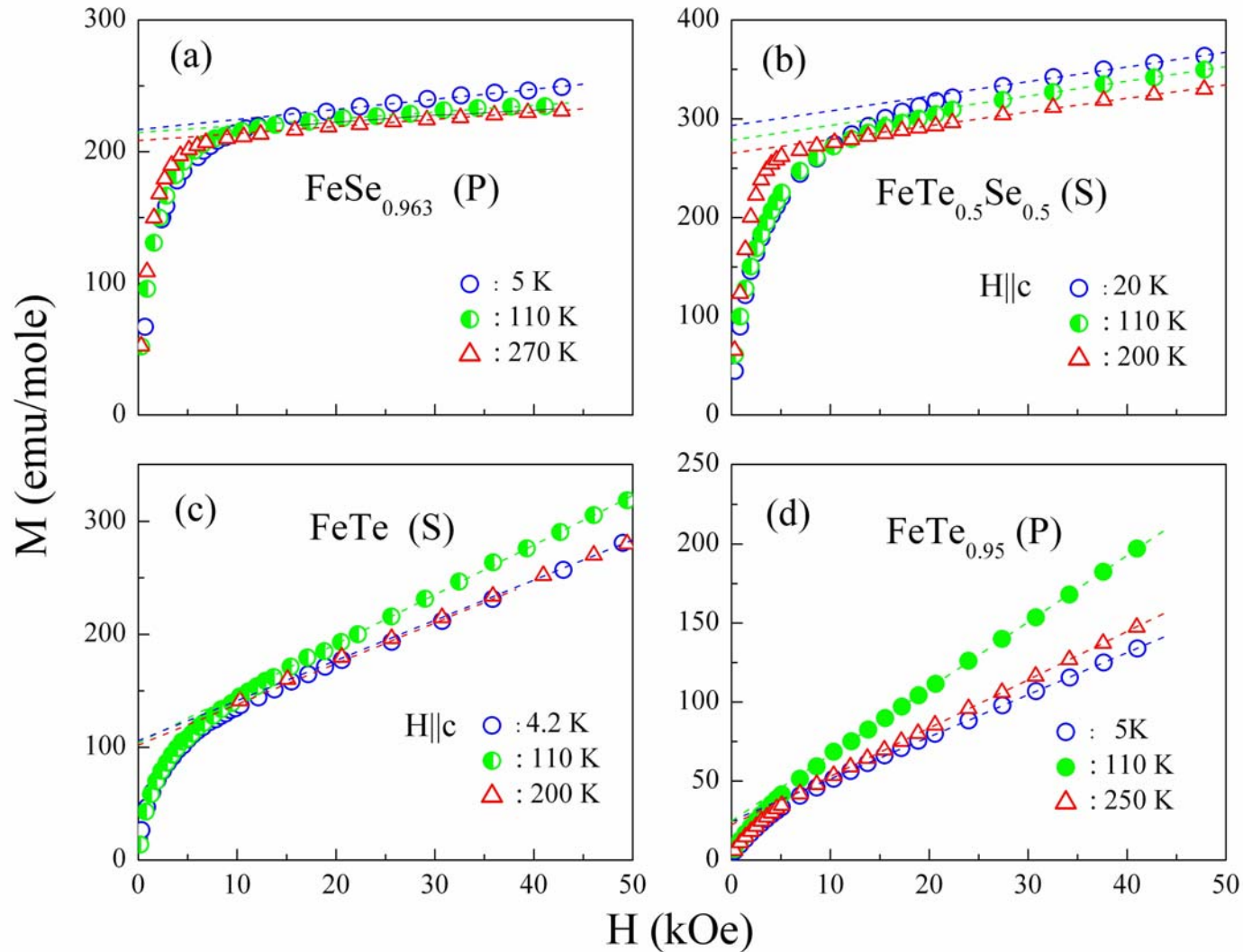
- V-shaped minimum and local maximum in DOS(E) in vicinity of E_F can govern magnetic properties of LaFeAsO under fluorine doping and/or oxygen deficiency.
- A substantial and puzzling growth of susceptibility with temperature is revealed in FeSe up to 300 K.
- The observed anisotropy of susceptibility is very large in FeSe, and comparable with the averaged susceptibility at low temperatures.
- Magnetic susceptibility in FeSe(Te) is found to increase gradually with Te content in about ten times.
- Ab initio calculations of paramagnetic susceptibility of LaFeAsO, FeSe and FeTe have revealed that these systems are in close proximity to quantum critical point.
- The strong positive pressure effect on χ is observed in FeSe and FeTe at low temperatures. At room temperature this effect is also strong, but *negative* in FeSe. The established large positive pressure effect on χ at low temperatures is related to the strong sensitivity of susceptibility to the height of Se (Te) species from the Fe plane, determining the dominant positive contribution to $d\ln\chi/dP$.
- Behavior of the superconducting transition temperature of FeSe with pressure correlates with density of electronic states at Fermi level.

Phase diagram of FeSe system

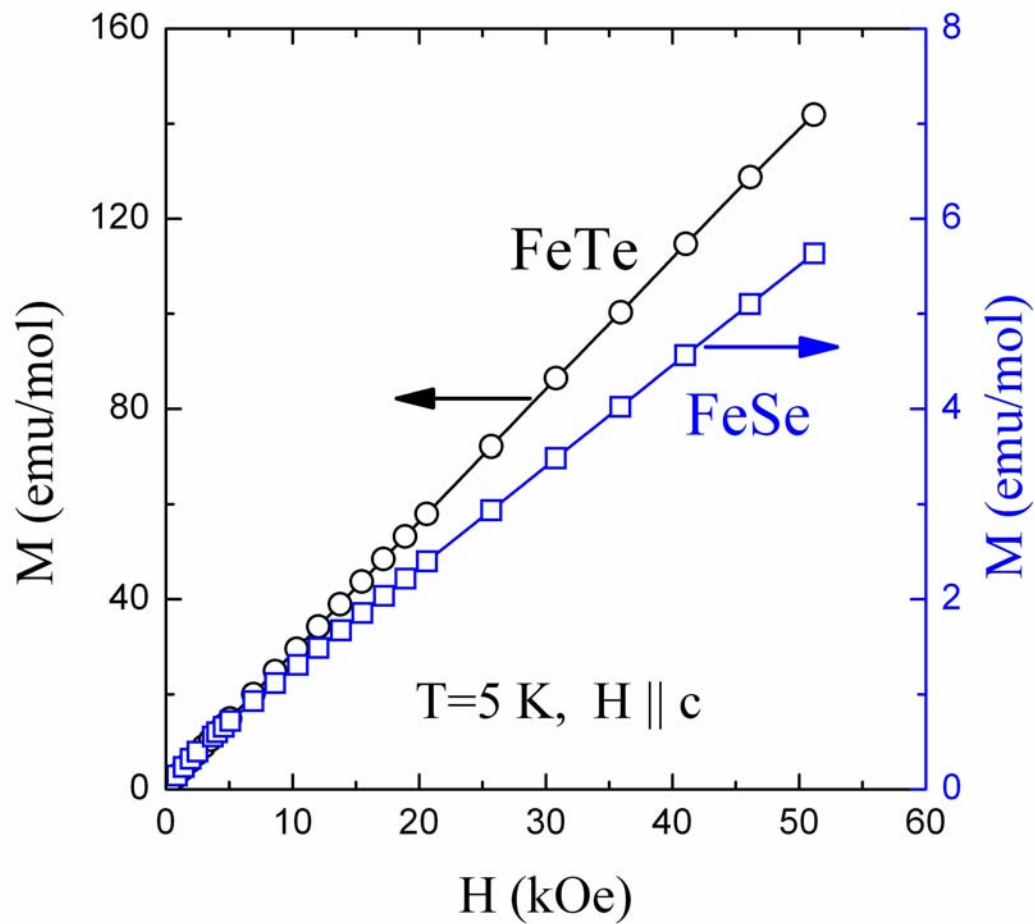
C. Petrovic et. al. Phys. Rev. B 83 (2011) 224502



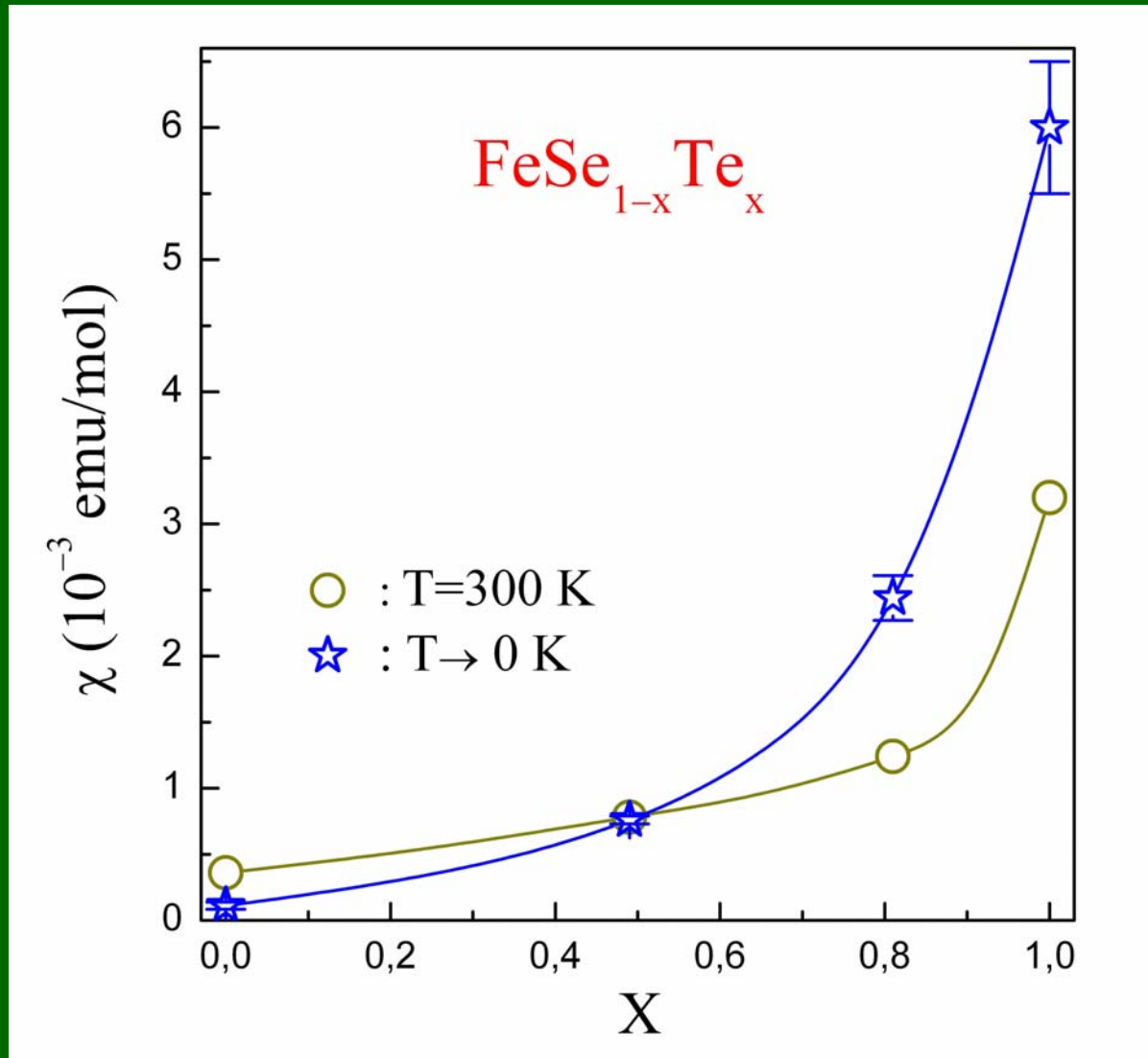
Magnetization of FeSe(Te)

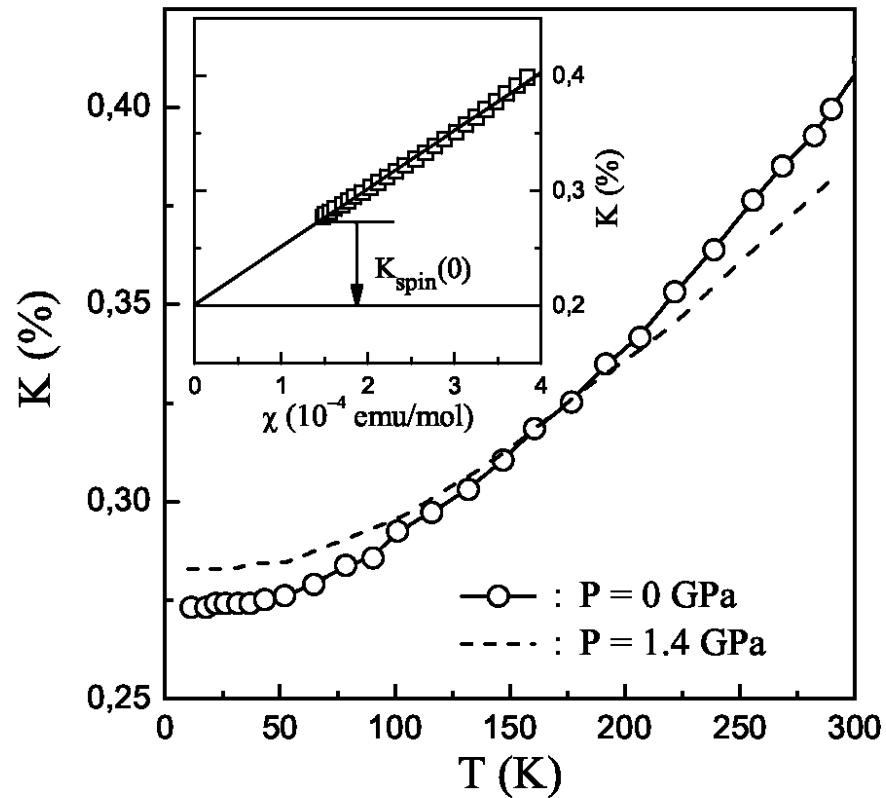


Magnetization of FeSe and FeTe



Concentration dependence of the magnetic susceptibility in FeSe(Te) at T=0 K and 300 K





Temperature dependencies of the NMR Knight shift K in FeSe measured at ambient pressure (—○—) and at $P=1.4$ GPa (dashed line). The inset shows dependence of K on the averaged magnetic susceptibility for FeSe.

Magnetic susceptibility χ (in 10^{-3} emu/mol) and its pressure derivative $d \ln \chi / dP$ (Mbar^{-1}) at different temperatures for polycrystalline $\text{FeTe}_{0.95}$ and single-crystalline FeTe compounds.

		$\text{FeTe}_{0.95}$	FeTe
χ	55 K	2.65	2.78
	78 K	4.53	5.19
	300 K	2.82	3.20
$\frac{d \ln \chi}{dP}$	55 K	28.4 ± 1.5	30 ± 1.5
	78 K	23.8 ± 1.5	22.3 ± 1.5
	300 K	14.4 ± 0.5	12.6 ± 0.5